Multi-level detection of damaged buildings from high-resolution optical satellite images

T. Thuy Vu[*a], Masashi Matsuoka[b], Fumio Yamazaki[a]
[a]Chiba University, 1-33 Yayoi-cho, Inage-ku, Chiba, 263-8522, Japan;
[b]Earthquake Disaster Mitigation Research Center, 1-5-2 Kaigandori, Wakinohama, Chuo-ku, Kobe, 651-0073, Japan

ABSTRACT

This paper presents a newly developed multi-level detection methodology using high-resolution optical satellite images. It aims to balance the quick response requirement and the details of detected results and hence, to satisfy various user demands. Damage extent is firstly detected from only post-disaster image on the first level, texture-based processing. This level quickly maps the damage extent and damage distribution but not in details. In some focused areas, the second level with object-based processing will derive further details of the damage using both pre- and post- data. The methodology is demonstrated on QuickBird images acquired over the damage areas of Bam, Iran, which was extensively devastated by the December 2003 earthquake. The detected results show a good agreement with the ones by visual detection and field survey.

Keywords: earthquake, damage detection, high-resolution satellite image, object-based, texture-based processing

1. INTRODUCTION

Time is a critical factor in post-disaster response. Making use of remotely sensed data is a good solution to reduce the time of gathering information. This kind of data is especially useful for the hard-hit and difficult-to-access areas. Recent catastrophes have been observed and captured by various remote sensors on different space-borne or airborne platforms. It triggers a great employment of remote sensing techniques in post-disaster response. Focusing on the employment of remote sensing in earthquake damage detection, many researches and implementations have been carried out after several recent earthquakes such as the 1995 Kobe, Japan earthquake[1], the 1999 Kocaeli, Turkey earthquake[2,3], the 2001 Gujarat, India earthquake[4,5], the 2003 Bam, Iran earthquake[6,7], the 2006 Central Java earthquake[8,9]. Either optical or radar, images at different resolutions have been used. The availability of higher resolution images such as QuickBird and Ikonos these days allows the interpretation of damage scale of each building block or even each individual building rather than overall damage distribution and damage extent. However, those high-resolution satellite images introduce higher internal variability and noise within land-use classes. They cause more difficulties in handling the data. Both visual and automated interpretations are used to derive the damage information from remotely sensed images. Reducing the processing time is also in serious concern.

At the lowest level of processing, image processing deals with pixels. Each pixel possesses the gray value that represents the spectral reflectance at its location. Based on that, a vast amount of pixel-based algorithms were developed. Texture-based algorithms are higher level of processing, which analyze different kinds of relationship among the neighbors of each pixel. These two types of processing have been successfully used for coarse resolution images like Landsat and ERS[1,2,3]. The reason is that coarse images do not provide detailed information. A pixel itself might be a mixture of different objects. Therefore, pixel or texture information is the reasonable cue for the detection and extraction of damage extent and distribution. Those pixel-based and texture-based methods developed could be used with airborne-based images[4] and high-resolution satellite images[6]. However, it was unable to exploit all possessed information in a high-resolution image. The visual interpretation, which obviously is time-consuming and requires experienced interpreters, has been a more reliable method[7]. To derive more detailed information, which is contained in an airborne-based image or a high-resolution satellite image such as QuickBird and Ikonos, requires much more complicated processing.

[*] thuyvu@as.tu.chiba-u.ac.jp; phone 81-43-290-3557; http://ares.tu.chiba-u.jp/

Disaster Forewarning Diagnostic Methods and Management, edited by Felix Kogan,
Shahid Habib, V. S. Hegde, Masashi Matsuoka, Proc. of SPIE Vol. 6412, 64120O, (2006)
0277-786X/06/$15 · doi: 10.1117/12.693846

To fully exploit detailed information on high-resolution satellite images and also to be adopted for quickly response after a catastrophe, we develop a multi-level damage detection method. On the first level, a simpler texture-based detection[6] is employed over a large extent to quickly detect damage extent and distribution. Observing the behavior of edge texture, this level successfully point out the "hot spot" of damage and totally collapsed buildings. Based on a "hot spot" of concern, its patch is generated and passed to an object-based detection for more detailed information on the second level. Two QuickBird images acquired over Bam city, Iran before and after the earthquake on December 26, 2003 are used for demonstration. Section 2 of this paper will briefly describe the texture-based detection. A newly developed object-based damage detection method is introduced in Section 3. It is followed by the discussion on the detected results and further development (Sections 4 and 5).

2. TEXTURE-BASED PROCESSING

On this first level, we employed the texture-based algorithm developed for processing aerial photograph[4]. It was also further developed for applying on high-resolution satellite images[6]. More details of the algorithm are referred to these publications of our previous works. Briefly, the edge intensity (*Ei*) is derived from a 7x7 Prewitt filter on the intensity (brightness) image. *Ei* is obtained from the maximum value in the templates for eight directions on the edges. An edge direction is defined as the direction of *Ei*, such as 0 - 180, 45 - 225, 90 - 270, and 135 - 315 degrees. Using the *Ei* value, *Ev* is calculated as a variance in a 7 x 7 pixel window. The ratio of the predominant direction of the edge elements in a 7 x 7 pixel window, *Ed*, is also calculated. Subsequently, the co-occurrence textures, the angular second moment (*Ta*) and entropy (*Te*), are calculated in a 7 x 7 pixel local area.

Both textures represent the uniformity of the edge structure but have opposite trends. Collapsed buildings should show the strongest trends of non-uniformity, i.e. lowest range of *Ta* and highest range of *Te*. Table 1 shows the threshold values for the above-mentioned parameters. Finally, the local density in 31 x 31 pixel window of the detected pixels are assessed to remove the meaningless spots.

Table 1. Threshold values for indices.

Index	Threshold values
Ev: edge variance	2.0 - 6.8 ($\times 10^{5}$)
Ed: edge direction	0.3 - 0.6
Ta: angular second moment	0.75 - 6.6 ($\times 10^{-2}$)
Te: entropy	3.5 - 4.2

Several pre-processing steps are required prior to applying the above algorithm on high-resolution satellite images. First, pan-sharpening is carried out to exploit the multi-spectral information at the better resolution of panchromatic band. Here, we employed our improved pan-sharpening algorithm, which is based on color-normalized method and includes a histogram stretching to match the pan-sharpen channels with original multi-spectral channels. Second, the histograms of these pan-sharpened bands are modified to match that of a natural color photo. This step is to simulate a satellite image look as an aerial photograph. It is very important because we utilize the threshold values successfully used for the aerial photograph. Then, the intensity image is generated and the abovementioned texture-based algorithm can be employed. Vegetation might be removed in advance by thresholding the Normalized Difference Vegetation Index (NDVI). This helps to improve the detection accuracy due to the similarity of vegetation textures and collapsed area textures.

Post-disaster QuickBird image acquired on January 03, 2004 over the hard-hit areas of Bam city, Iran is shown in Fig.1. The result of texture-based detection is represented as black spots overlain on this true-color-composite QuickBird image (Fig. 2). Visual inspection showed that most of areas of damage buildings were successfully detected.

Fig. 1. True-color-composite QuickBird image of Bam, Iran acquired on January 03, 2004.

Fig. 2. Texture-based detected results shown as black spots on QuickBird image.

3. OBJECT-BASED PROCESSING

A small area in this hard-hit area of Bam was chosen for demonstrating the object-based processing. Texture-based processing detected that 37.9% of the area was damaged. Since buildings dominated in the area, it can be said approximately that 37.9% buildings were damaged. In object-based processing, both pre-disaster and post-disaster information are required. Perhaps, existing GIS database can provide the pre-disaster information. However, it was not the case of Bam, Iran. Thus, we purchased the QuickBird image acquired on September 30, 2003. Selected areas from these pre- and post- images are shown in Fig. 3.

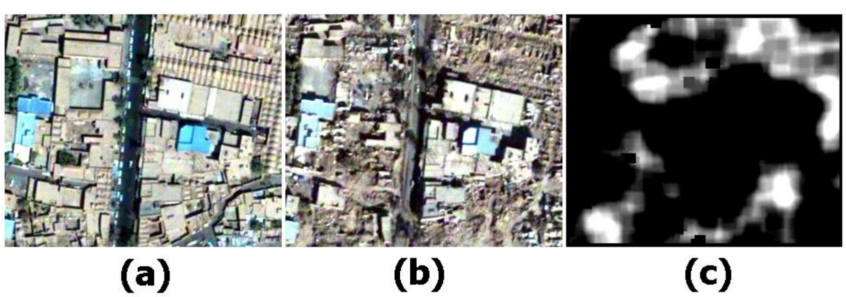

Fig.3. The pre- (a), post- (b) QuickBird images of the study area, and (c) texture-based detected result in bright color.

Our object-based processing was developed based on an area morphology[10] multi-scale framework. Early development and preliminary results were recently published[11,12]. How to generate a scale-space based on area morphology was presented in those publications. This paper discusses more on the classification and extraction across the scale-space. After generating the scale-space, the step-by-step processing is as follows.

First, on each scale, spectral information is categorized into different classes by K-mean clustering. Separately clustered on each scale, the spectral indices across the scale-space of the same class might be different. To be further used in extraction, the same class should be re-assigned to the same index.

The correlation analysis, which measures the similarity between the distribution histograms of each class on the original image, is employed to find out the best match with the finest scale as the reference. Let $H_{i,0}$ is the histogram of class i on the finest scale and $H_{j,k}$ is the histogram of a class j on the scale k. Their correlation is computed as follow.

$$\rho(i,j,k) = \frac{cov(H_{j,k}, H_{i,0})}{std(H_{j,k}) \times std(H_{i,0})} \tag{1}$$

where cov is the covariance of these histograms and std is the standard deviation of each histogram. The correlation values of histogram of class j on the scale k with every class on the finest scale are computed. The maximum value shows the best match and this class index on the finest scale replaces class j on the scale k.

Next, the objects are assigned their ID on each scale and can be linked across the scale-space through the same spectral index. Prior to the extraction of an object, it is recommended to eliminate the possible duplicate existence on two consecutive scales. Due to the complex scene of an urban area, this situation often occurs. Three criteria are taken into account. First, an object on the finer scale (object A) overlapping an object on the next coarser scale (object B) is investigated. Second, if the center of object A is not so far the one of object B (a distance of 3 pixels, for example), their areas are computed and compared. If object A's area is approximate object B's area (80% difference), the object A is removed as it is the duplicate of object B. A range of spectral indices and a range of scales relevant to building features are chosen for an extraction across the scale-space from the finest to the coarsest scales. Fig. 4 shows the extracted building features from the pre- and post- images. The building features are shown in different colors according to their ID numbers.

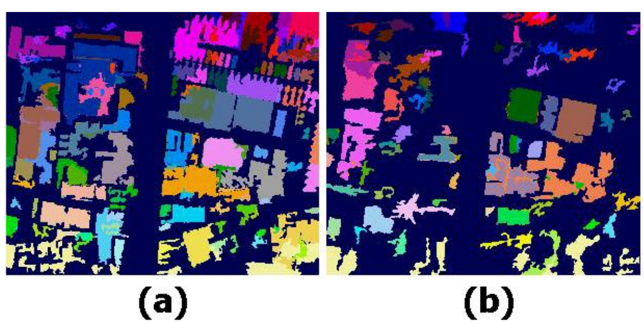

Fig. 4. Object-based extracted building features from the pre- (a) and post- (b) images.

Finally, extracted building features from the pre- and post- images are compared to map the damaged buildings. A building is defined as damaged one if its area reduced more than an area threshold. The possibility to successfully locate the partly collapsed buildings highly depends on the selection of this threshold. Damaged buildings were detected from Bam images are shown in Fig. 5. The result found that 116 of 151 buildings were damaged.

4. DISCUSSION

Exploiting more information contained in an image, object-based processing obviously takes longer computational time than texture-based processing. Complex processing might produce the required details but also produce a messy scene of extracted building features. It depends on the characteristics of the focused area and the satellite images. For instances, the uniform spectral reflectance of building features in Bam city caused the difficulties in exactly extracting the building boundaries. As a result, it was very difficult to compare building-by-building between the pre- and post- images. Thus, it was unable to exactly count the number of damaged buildings and verify the damage grades.

The texture-based detected result is represented as semi-transparent polygons overlain on the object-based detected results (Fig. 5) to crosscheck the results between two levels. This texture-based result is also overlain on the pre- and post- images for references in this figure. Fig. 5 shows that level 1 result covered most of totally collapsed areas. Level 2, on the other hand, detected both totally and partly collapsed buildings since it concerned objects not pixels. The comparison here also concluded that the texture-based results should be represented at a less detailed scale.

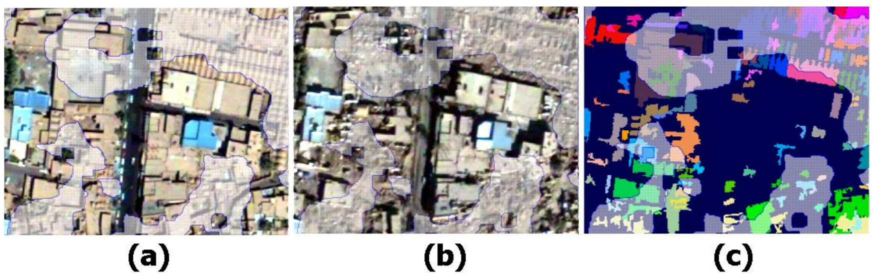

Fig. 5. The texture-based detected result overlain on the pre- (a), post- (b) images, and the object-based damage detected result (c).

We investigated further the object-based detected results with the one by visual damage detection[7]. The visual inspection classified damaged buildings according to European Macroseismic Scale (EMS), i.e. 5 grades of damage. Object-based detection produced a good agreement with Grade 4 and 5 damaged buildings (Fig. 6). Some other grade 3 and 4 points located in non-damage areas detected by object-based method. However, parts of these buildings were detected as shown in red circle in Fig. 6. Fig. 6 also presents the difficulties in detection of exact boundaries of the buildings even by visual interpretation.

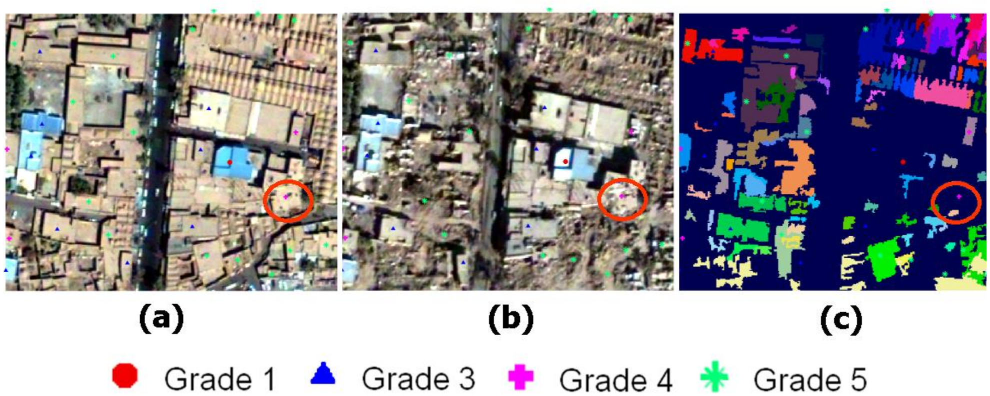

Fig. 6. Compare the visual interpretation results (color dots) and the pre- (a), post- (b) images and (c) object-based detected results.

5. CONCLUSION

Multi-level damage detection was proposed to flexibly satisfy diverse user demands in post-disaster response. Level 1 can quickly produce the damage distribution to help the public figure out the extent of damage. Level 2 assists the investigation in more details to determine the level and quantity of damage in some small areas of specific concern. Multi-level mechanism also helps to reduce the cost including data acquisition cost and computational cost. It is recommended that the developed multi-level damage detection methodology should be further tested in various areas. A multi-level damage detection system should be developed for widely and easy-to-use in the future.

6. ACKNOWLEDGEMENT

The QuickBird images used in this study are owned by Digital Globe, Inc. The images of Bam, Iran are licensed and provided by Earthquake Engineering Research Institute (EERI), Oakland, California, USA.

REFERENCES

1. M. Matsuoka and F. Yamazaki, "Characteristics of Satellite Images of Damaged Areas due to the 1995 Kobe Earthquake," *Proc. of 2nd Conference on the Applications of Remote Sensing and GIS for Disaster Management*, The George Washington University (1999).
2. R.T. Eguchi, C.K. Huyck, B. Houshmand, B. Mansouri, M. Shinozuka, F. Yamazaki and M. Matsuoka, "The Marmara Earthquake: A View from space: The Marmara, Turkey Earthquake of August 17, 1999: Reconnaissance Report," *Technical Report MCEER-00-0001*, 151-169 (2000).
3. M. Estrada, F. Yamazaki and M. Matsuoka, "Use of Landsat Images for the Identification of Damage due to the 1999 Kocaeli, Turkey Earthquake," *Proc. of 21st Asian Conference on Remote Sensing*, 1185-1190, Singapore (2001).
4. H. Mitomi, J. Saita, M. Matsuoka and F. Yamazaki, "Automated Damage Detection of Buildings from Aerial Television Images of the 2001 Gujarat, India Earthquake," *Proc. of the IGARSS 2001*, IEEE, CD-ROM, 3p (2001).
5. K. Saito, R.J.S. Spence, C. Going and M. Markus, "Using high-resolution satellite images for post-earthquake building damage assessment: a study following the 26 January 2001 Gujarat Earthquake," *Earthquake Spectra*, 20 (1), 145–169 (2004).
6. T.T. Vu, M. Matsuoka and F. Yamazaki, "Detection and Animation of Damage Using Very High-resolution Satellite Data Following the 2003 Bam, Iran, Earthquake" *Earthquake Spectra*, 21 (S1), S319-S327 (2005).
7. F. Yamazaki, Y. Yano and M. Matsuoka, "Visual Damage Interpretation of Buildings in Bam City Using QuickBird Images Following the 2003 Bam, Iran, Earthquake," *Earthquake Spectra*, 21 (S1), S329-S336 (2005).
8. M. Matsuoka and F. Yamazaki, "Use of SAR Imagery for Monitoring Areas Damaged Due to The 2006 Mid Java, Indonesia Earthquake," *Proc. of 4th International workshop on Remote Sensing for Post-Disaster Res*ponse, Cambridge, United Kingdom (2006).
9. K. Matsumoto, T.T. Vu and F. Yamazaki, "Extraction of damaged buildings using high resolution satellite images in the 2006 Central Java Earthquake," *Proc. of ACRS 2006*, Ulaanbaatar, Mongolia (2006).
10. L. Vincent, "Morphological Area Opening and Closings for Greyscale Images," *Proc. NATO Shape in Picture workshop*, Driebergen, The Netherlands, Springer-Verlag, 197-208 (1992).
11. T.T. Vu, M. Matsuoka and F. Yamazaki, "Preliminary results in Development of an Object-based Image Analysis Method for Earthquake Damage Assessment," *Proc. of 3rd International workshop on Remote Sensing for Post-Disaster Response*, Chiba, Japan (2005).
12. T.T. Vu, M. Matsuoka and F. Yamazaki, "Towards object-based damage detection," *Proc. of ISPRS workshop DIMAI'2005*, Bangkok, Thailand (2005).